Exciton spectra of KCN and $K(CN)_xCl_{1-x}$ crystals. Exciton-vibron coupling in ordered and disordered systems

M. Rossinelli* and M. Bösch†
Laboratory of Solid State Physics, Swiss Federal Institute of Technology, CH-8092 Zürich, Switzerland

G. Zumofen
Laboratory of Physical Chemistry, Swiss Federal Institute of Technology, CH-8092 Zürich, Switzerland

(Received 31 March 1980)

The reflectance spectra of KCN and $K(CN)_xCl_{1-x}$ crystals have been measured in the energy range from 5 to 11.5 eV at temperatures between 5 and 300 K. In KCN seven vibrational bands of the $A\ ^1\Pi \leftarrow X\ ^1\Sigma^+$ transition of the CN^- ion appear above 6.8 eV. Below 80 K a resolved splitting of the exciton bands is observed. The effects of exciton-phonon coupling and of the reorientational motion of the CN^- ions on the reflectance bands are discussed. Other optical transitions occurring at higher energies are interpreted on the basis of a simple electronic energy-level scheme. In $K(CN)_xCl_{1-x}$ mixed crystals the Wannier excitons of chlorine and the vibronic excitons of CN^- are observed throughout the whole composition range. The concentration dependence of the $A\ ^1\Pi$ exciton progression is discussed in terms of a point-dipole lattice model. The observed inhomogeneous line broadening of the $A\ ^1\Pi$ transition originating either from orientational disorder above 80 K or from nonequivalent molecular environments in mixed crystals is compared with the one derived from simulation calculations.

I. INTRODUCTION

The alkali cyanides are suitable compounds for the investigation of disorders in molecular crystals. KCN and NaCN are examples of orientationally disordered crystals and have been studied extensively by various methods.[1-11] At higher temperatures the CN^- ions are reorienting independently among several equilibrium directions, thereby destroying the translational symmetry of the lattice. With decreasing temperature the degree of orientational order increases as the crystals undergo phase transitions.

The study of electronic excitations in these solids is therefore of interest with regard to the general problem of the electronic structure of disordered materials. The reflectance spectrum of crystalline KCN around 7 eV displays a progression of exciton states due to the $A\ ^1\Pi \leftarrow X\ ^1\Sigma^+$ electronic transition of the CN^- molecule coupled with vibrational transitions. Other reflectance bands are observed between 8 and 11.5 eV.[12,13] In this work we report and discuss reflectance measurements on pure KCN as a function of temperature in the range from 5 to 300 K. Based on the interpretation of the low-temperature KCN spectrum given in Ref. 13 we analyze the temperature dependence of the $A\ ^1\Pi$ excitonic progression by taking into account exciton-phonon coupling as well as the effects of orientational disorder upon the exciton states. An interpretation of the optical transitions observed at higher energies is given in terms of a band-structure scheme.

Since compositional or substitutional disorder also affects the electronic structure of solids we extended our investigation to the $K(CN)_xCl_{1-x}$ system. It has the outstanding property that x can be varied continuously over the whole composition range. Special attention is focused on the concentration dependence of the $A\ ^1\Pi \leftarrow X\ ^1\Sigma^+$ exciton progression. The experimental results are discussed in connection with the theory of molecular excitons.

II. CRYSTAL STRUCTURES AND PHASE TRANSITIONS

Above 168 K, potassium cyanide has an average structure of the NaCl-type with the CN^- ions reorienting among several equilibrium directions.[4] A first-order phase transition to a partially ordered orthorhombic structure (space group D_{2h}^{25}) occurs at 168 K. The CN^- ions align along the axis close to the [110] axis of the original cubic structure, but stay disordered with respect to the CN or NC sequence and hence with respect to the sign of their electric dipole moment.[1-3] The transition is due to an interaction between the CN^- groups mediated by the lattice strain that favors parallel or antiparallel orientation.[8,14]

Below 168 K the crystal breaks up into crystallographic domains corresponding to the six equivalent [110] directions of the cubic phase.[2,11] Heat-capacity measurements,[3] Raman spectroscopy,[5,6] and neutron scattering[10] indicate that a second-order phase transition occurring at 83 K leads to an antiferroelectric ordering of the CN^-

ions. The space group of this phase is presumably D_{2h}^{13} according to Ref. 6 (Fig. 1). This assignment, however, has been questioned in a recent paper.[15]

A simple model that describes the reorientational motion of the CN^- ions was proposed by Suga *et al.*[3] At the lowest temperatures the cyanide ions are aligned along the *c* axis of the orthorhombic unit cell and librate around their equilibrium orientations. The directions will now be referred to the orthorhombic axis. The energy difference *W* between the [001] and [00$\bar{1}$] orientations (CN and NC sequence) arises from the electrostatic interaction of the dipole moment of the CN^- ion with the local electric field produced by all the surrounding dipoles. With increasing temperature the flipping motion between the two orientations is gradually excited and the energy difference *W* diminishes, until at 83 K the two orientations are energetically equivalent (a disordered state).

A different model was proposed later to explain EPR (Refs. 11 and 15) and dielectric[9] measurements. In the partially ordered orthorhombic phase above 83 K, the CN^- groups are rapidly reorienting in a ten-well crystal potential with minima corresponding to the [001] and [111] directions. The two equivalent [001] and [00$\bar{1}$] orientations are preferred owing to the lower potential energy.

The inversion of the electric dipole moment is thought to be achieved through intermediate [111] orientations (see Fig. 2). Again, below 83 K the potential is gradually modified by the electrostatic interaction energy $-\vec{p}\vec{E}_{loc}$ so that the [001] and [00$\bar{1}$] orientations are no longer equivalent. This leads to antiferroelectric ordering (Fig. 1).

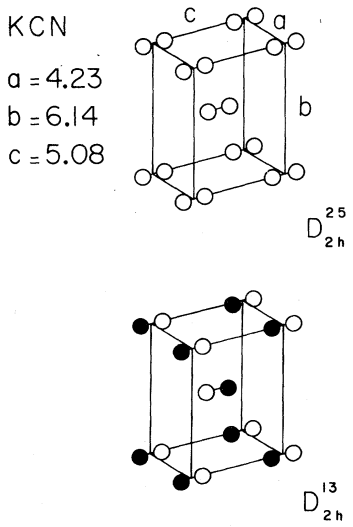

FIG. 1. Structure of the low-temperature phases of KCN. Lattice parameters according to Ref. 2.

III. EXPERIMENTAL TECHNIQUES

A. Crystal growth

The crystals were grown from the melt in a closed Czochralski furnace starting with reagent-grade materials. Owing to the high reactivity of the cyanides we used helium as a protective atmosphere. The anion purity in the crystals was better than 99.6% as determined by argentometric titration. The only anion impurities detected by infrared spectroscopy were OCN^- and CO_3^{2-}. KCN crystals are hygroscopic; therefore all preparation steps were carried out in a glove box filled with pure helium.

B. Reflectance measurements

Nearly-normal-incidence reflectance spectra were taken in an oil-free vacuum ultraviolet spectrometer system built around a McPherson 225 grating monochromator.[16] The light source was a Hinteregger-type capillary discharge lamp (McPherson model 630); hydrogen gas was used in the discharge. Most spectra were measured with a 1200-grooves/mm grating blazed at 1500 Å and with the entrance and exit slits of the monochromator at a constant width of 250 μm, corresponding to a resolution of 2.2 Å. The angle of the light beam incident upon the sample surface was 12°.

Crystals of about $4 \times 4 \times 4$ mm^3 attached with epoxy resin to a copper sample holder were cleaved *in situ* at pressures below 5×10^{-7} Torr prior to the measurements in order to minimize surface contamination. Liquid-helium temperatures can be reached 10 min after cleaving by means of a continuous flow evaporation cryostat in which the temperature can be varied between 5 and 400 K. The temperature was measured with a carbon resistor and with a thermocouple firmly

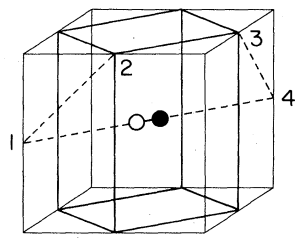

FIG. 2. Equilibrium positions and reorientation paths of the CN^- ions in KCN. According to Ref. 3: two-well potential with equilibrium orientations 1 and 4. According to Refs. 9 and 11: 10-well potential; a possible reorientation path is $1 \rightarrow 2 \rightarrow 3 \rightarrow 4$.

attached to the sample holder in the immediate vicinity of the sample, and was stable to within 0.05 K. During the measurements a liquid-nitrogen cold trap surrounding the cold finger of the cryostat lowered the pressure of condensable gases. Data were taken at pressures of 4×10^{-8} Torr.

Upon cooling, stresses can appear in the crystal both as a consequence of gluing it to the sample holder and because of the formation of crystallographic domains. These stresses may influence the structures observed in the spectra. We have measured for comparison a KCN crystal mounted without the use of epoxy resin. In the reflectance spectrum at 5 K no difference could be detected, which indicates that the effect of the resin is very small. It is possible that slips and twinnings occurring at the domain boundaries in the low-temperature phases act to reduce the internal strains.[2]

IV. POTASSIUM CYANIDE

A. Reflectance spectra

Reflectance spectra of pure KCN are shown in Figs. 3 and 4. Room-temperature data are reproducible to within 2–3%. Measurements at low temperatures, however, are problematic. When cooled through the 168-K transition the crystals become opaque because of the formation of domains, and the reflectance is reduced by light scattering. The intensity of the scattering depends in a complicated way upon the size of the domains [typically 4000 Å (Refs. 2 and 3)] and upon the frequency of the incident light. Since at low temperature the surface quality varies from sample to sample, absolute reflectance values also vary and are of limited accuracy. The global decrease of the reflectance above 5 eV (Fig. 3) is probably due to the increase of the scattering with increasing photon energy.

The reflectance spectra around 7 eV show a progression of clearly resolved bands due to the transitions from the $X\,^1\Sigma^+$ ground state of the CN^- molecule to the different vibrational levels of the $A\,^1\Pi$ excited electronic state (Fig. 4). Similar exciton progressions are observed in the spectra of solid N_2 (Ref. 17) and CO.[18] At 5 K the perturbation of the excited $A\,^1\Pi$ state by the crystal field results in a splitting of each vibrational band into two components. The weak band at 7.14 eV is assigned to a two-particle state. A detailed discussion of the $A\,^1\Pi$ exciton progression is given in Sec. VI. The reflectance bands observed between 8.5 and 11.5 eV are probably due to higher electronic transitions of the CN^- ion and to charge-transfer excitons.

B. Kramers-Kronig analysis

The complex dielectric function

$$\hat{\epsilon}(\omega)=\epsilon_1+i\epsilon_2=(n^2-k^2)+2ink \qquad (1)$$

can be obtained from the reflectance data by means of the Kramers-Kronig integral transform. In our case the experimental data extend to 11.5 eV only so that the evaluation method proposed by Roessler was used.[19,20] This method does not rely upon extrapolations of the data throughout the unmeasured energy range. The contribution from this region to the phase change θ on reflection is determined by the condition that θ must be zero at (any two) frequencies in the spectral range where the crystal is transparent, in this case below 4 eV.

The evaluation of $\hat{\epsilon}(\omega)$ for the untwinned cubic phase is straightforward (Fig. 5). The analysis of the low-temperature spectrum, however, often yields negative values of the extinction coefficient k. This unphysical result is due to the decrease of the reflectance above 5 eV through scattering by domains. In order to obtain at least a reasonable estimate of $\hat{\epsilon}(\omega)$ at 5 K the low-energy

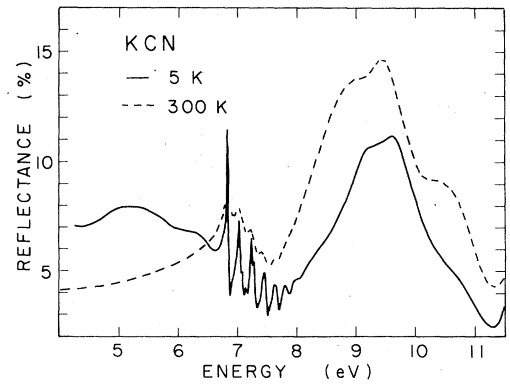

FIG. 3. Reflectance spectrum of KCN at room temperature (dashed line) and at 5 K (solid line). See the Appendix for details.

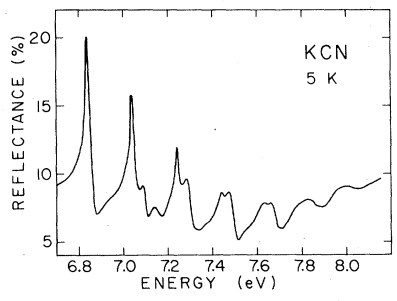

FIG. 4. Reflectance spectrum of the $A\,^1\Pi \leftarrow X\,^1\Sigma^+$ progression in KCN at 5 K.

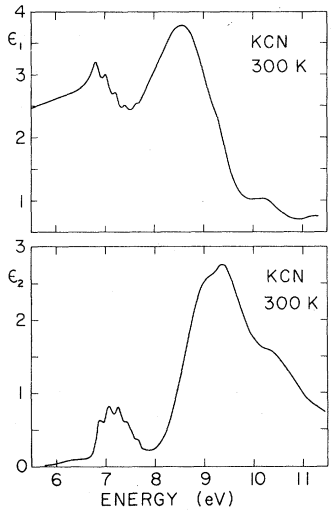

FIG. 5. Dielectric functions ϵ_1 and ϵ_2 of KCN at room temperature, as derived from a Kramers-Kronig analysis of the reflectance data.

part of the spectrum was approximated by properly shifting the reflectance curve taken at room temperature. The results are given in Fig. 6.

C. Discussion

From the analogy with KCl and with the alkali halides in general we expect the upper valence bands of KCN to be mainly constructed out of the electronic states of the anion. A qualitative energy-band diagram can be obtained within the tight-binding approximation using the symmetry properties of the crystal.[21,22]

The electronic structure of the CN^- ion in its ground state is[23-26]

$$(1\sigma)^2(2\sigma)^2(3\sigma)^2(4\sigma)^2(1\pi_{x,y})^4(5\sigma)^2(2\pi_{x,y})^0(6\sigma)^0 : X\,^1\Sigma^+ .$$

As in the isoelectronic CO molecule we assume for the lowest excited states the following electronic configurations and the corresponding molecular states[27]:

$$\cdots(1\pi_{x,y})^4(5\sigma)^1(2\pi_{x,y})^1 : A\,^1\Pi, a\,^3\Pi$$

$$\cdots(1\pi_{x,y})^3(5\sigma)^2(2\pi_{x,y})^1 : {}^1\Sigma^+, {}^1\Sigma^-, {}^1\Delta,$$
$${}^3\Sigma^+, {}^3\Sigma^-, {}^3\Delta .$$

Some properties of the free CN^- ion are listed in Table I.

In the ordered phase below 83 K (space group D_{2h}^{13}) the primitive orthorhombic unit cell contains two K^+ ions and two CN^- ions aligned along the c axis. We consider the molecular orbitals $\phi_n(\vec{r})$ localized on the molecule at $\vec{d}_\mu$ in the unit cell and construct the Bloch sums

$$\Phi_n^{(\mu)}(\vec{k},\vec{r}) = \frac{1}{\sqrt{N}} e^{i\vec{k}\cdot\vec{d}_\mu} \sum_{\vec{\tau}_\nu} e^{i\vec{k}\cdot\vec{\tau}_\nu} \phi_n(\vec{r} - \vec{d}_\mu - \vec{\tau}_\nu), \tag{2}$$

where $\vec{\tau}_\nu$ is a lattice translation vector. The crystal wave functions $\Psi_v(\vec{k},\vec{r})$ of the different bands v can be expanded in the set given in Eq. (2) as follows:

$$\Psi_v(\vec{k},\vec{r}) = \sum_{n,\mu} a_{n_\mu}(\vec{k}) \Phi_n^{(\mu)}(\vec{k},\vec{r}) . \tag{3}$$

The number of coefficients $a_{n_\mu}(\vec{k})$ is reduced by requiring that the functions Ψ_v be partner functions of one of the irreducible representations of the group of the vector $\vec{k}$. Symmetrized combinations of Bloch functions at the Γ point are given in Table II. The electronic states of the crystal are then classified according to the irreducible representations of the group of $\vec{k}$.

Figure 7 represents a schematic band structure. We anticipate valence bands arising from the 4σ, 1π, and 5σ molecular orbitals, followed toward higher energies by the empty 2π bands. Conduction bands arising from the potassium $4s$ and $3d$ orbitals are expected in analogy with the alkali halides, perhaps with a contribution from the CN^- 6σ orbitals. We notice that at point Γ ($\vec{k}=0$) and Z [$\vec{k}=(0, 0, \pi/c)$] all the irreducible representations of the group of $\vec{k}$ are one dimensional. Since the unit cell contains two identical CN^- molecules, the σ bands split into two subbands and the π bands into four subbands (Davydov splitting). At point X [$\vec{k}=(\pi/a, 0, 0)$] the allowed irreducible representations of the group of $\vec{k}$ are two dimensional and only the π_x-π_y splittings persist. The magnitude of the splittings and the exact order of the Davydov components

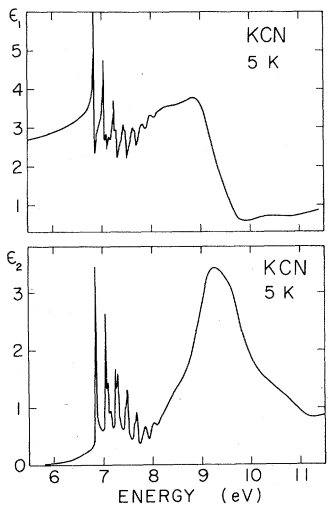

FIG. 6. Dielectric functions ϵ_1 and ϵ_2 of KCN at 5 K, as derived from the reflectance data.

TABLE I. Properties of the CN^- ion.

Permanent electric dipole moment:	$\mu(X\,^1\Sigma, v''=0)=0.63\times10^{-18}$ esu cm [a]	
	$\mu(A\,^1\Pi, v'=0)=0.47\times10^{-18}$ esu cm [a]	
Ionization potentials (IP) [b]:	Orbital	IP, eV
	5σ	10.2
	1π	11.5
	4σ	13.7

Transition energies (ground state $X\,^1\Sigma^+$) in eV:

$^1\Pi$		$^1\Delta$	$^1\Sigma^-$	$^1\Sigma^+$
5.69 [c]	4.69 [d]	7.46 [d]	7.46 [d]	9.27 [d]
11.5 [c]				16.2 [d]
12.4 [c]				19.1 [d]

Electron affinity: 3.17 eV [e]

[a] Reference 49: *Ab initio* SCF CI calculation.
[b] Reference 31: The values refer to the positions of the UPS peaks of solid NaCN. The effect of the cation is included.
[c] Reference 25: CNDO calculation of the free ion.
[d] Reference 26: Semiempirical SCF calculation of the free ion.
[e] *Handbook of Chemistry and Physics*, 57th ed. (Chemical Rubber, Cleveland, 1976).

have not been calculated.

The experimental work done so far on the ultraviolet properties of the CN^- ion includes absorption and emission measurements on CN^--doped alkali halides[28] as well as x-ray[29,30] and ultraviolet[31] photoelectron spectroscopy studies of KCN and NaCN. The $A\,^1\Pi \leftarrow X\,^1\Sigma^+$ vibronic progression is clearly observed in the uv absorption spectra of CN^- centers in alkali halides. In KCl:CN^-, the absorption maximum corresponding to the 0-0 transition occurs at 6.955 eV, close to the value of 6.951 eV for the electronic transition energy in pure KCN (Table IV). The transition energies calculated for the free ion (Table I) are much lower. Photoelectron spectra of NaCN (Ref. 31) show at low energies three peaks corresponding to ionization from the 5σ, 1π, and 4σ molecular orbital (MO). From the ionization potentials (10.2, 11.5, and 13.7 eV, respectively) one can deduce the approximate separations between the corresponding valence bands.

We can now attempt an interpretation of the optical transitions observed above 8 eV. At

TABLE II. Symmetrized combination of Bloch sums at point Γ and classification of the electronic states of the cystal (space group D_{2h}^{13}), where for brevity $\sigma^{(1)} \equiv \Phi_\sigma^{(1)}(\vec{k},\vec{r})$ [Eq. (2)].

	Γ	Λ	Σ	Z	X
$\Psi_\sigma^+ = \sigma^{(1)} + \sigma^{(2)}$	Γ_1^+	Λ_1	Σ_1	Z_1^+	X_1
$\Psi_\sigma^- = \sigma^{(1)} - \sigma^{(2)}$	Γ_3^-	Λ_1	Σ_4	Z_3^-	
$\Psi_{\pi_x}^+ = \pi_x^{(1)} + \pi_x^{(2)}$	Γ_4^-	Λ_2	Σ_1	Z_4^-	X_1
$\Psi_{\pi_x}^- = \pi_x^{(1)} - \pi_x^{(2)}$	Γ_2^+	Λ_2	Σ_4	Z_2^+	
$\Psi_{\pi_y}^+ = \pi_y^{(1)} + \pi_y^{(2)}$	Γ_2^-	Λ_4	Σ_2	Z_2^-	X_2
$\Psi_{\pi_y}^- = \pi_y^{(1)} - \pi_y^{(2)}$	Γ_4^+	Λ_4	Σ_3	Z_4^+	

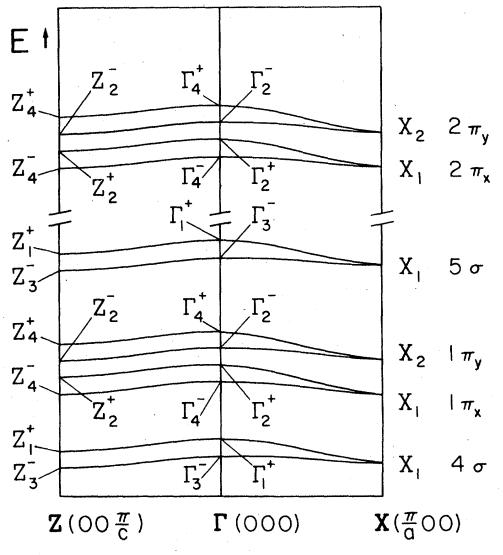

FIG. 7. Schematic band structure of KCN in the ordered phase below 83 K.

room temperature the reflectance spectrum consists of three broad and partly overlapping peaks centered at 9.0, 9.4, and 10.4 eV (Fig. 3). The ϵ_2 spectrum is similar. Upon cooling to 5 K the first two bands shift to higher energies (9.2 and 9.6 eV) while the third is somewhat obscured. On the whole the band shapes are only weakly temperature dependent, compared to the excitonic structures in the spectra of the alkali halides, which are characterized by a strong temperature dependence of the width and by sharp antiresonances on the high-energy side of the line-exciton peaks.

The first of these bands is likely to originate from transitions between the CN^- 5σ band and the lowest potassium conduction bands. Possibly the transitions are associated with charge-transfer excitons. An energy gap of about 9 eV is quite reasonable if compared to the corresponding value for KCl (8.7 eV). (The Madelung energies and the electron affinities of the anions in the two compounds are very close.) The bands at 9.4 and 10.4 eV are probably related to higher electronic excitations of the CN^- ions, corresponding to transitions between the occupied orbitals 4σ, 1π, and 5σ and the empty ones 2π and 6σ. The calculated transition energies for the free ion ($^1\Sigma^+ \leftarrow X^1\Sigma^+$ at 9.27 eV, $^1\Pi \leftarrow X^1\Sigma^+$ at 11.5 eV, see Table I) lie in this range. Furthermore, transitions of an electron from a bonding orbital (e.g., $5\sigma, 1\pi$) into the corresponding antibonding orbital ($6\sigma, 2\pi$) will result in large intensities.

V. MIXED CRYSTALS $K(CN)_xCl_{1-x}$

The optical spectra of substitutional binary solid solutions fall into two classes, the amalgamation and persistence types.[32] In the former the electronic structures corresponding to the two individual components are "amalgamated" to form a single structure, that of the mixed crystal or of the alloy. In the latter the electronic structures of the two components are observed simultaneously throughout the composition range. Model calculations by Onodera and Toyozawa[32] have demonstrated that when the difference Δ of the excitation energies of the individual components is large compared to the energy-band width the electronic structure of the mixed crystal will be of the persistence type. This is the case of the exciton spectra in halogen-substituted alkali halides, such as KCl-KBr,[33] where two separated exciton structures originating from the two constituent halogen ions are observed.

Figure 8 shows the reflectance spectra of $K(CN)_xCl_{1-x}$ mixed crystals between 6 and 11 eV. Our measurements on pure KCl are in good agreement with those reported in the literature.[34,35] In KCl the highest valence band arises from the Cl^- $3p$ atomic orbitals and is split by spin-orbit interaction into two subbands. At the Γ point the lowest conduction band is mainly built up of potassium s-like states. The two peaks observed in the reflectance at 7.78 and 7.92 eV are due to excitons bound to the highest valence band and to the lowest conduction band at Γ. The spin-orbit splitting of the halogen band (0.144 eV) is clearly resolved. Noteworthy is also the sharp antiresonance on the high-energy side of the doublet. The peak at 9.59 eV is assigned to an exciton bound to the upper valence band and to a conduction band minimum (built of potassium d-like states) at the X point. In the mixed system the vibronic excitons originating from the cyanide ions and the excitons associated with the chlorine ions are observed separately throughout the composition range. The spectra are thus typically of the persistence type, which emphasizes the "pseudo-alkali-halide" nature of crystalline KCN. The Γ excitons of chlorine shift to higher energies and the X excitons to lower energies as the cyanide concentration increases (Fig. 9). A similar shift is observed in the KCl-KBr system and is in agreement with the theory.[32] At the same time the disorder broadens the reflectance peaks so that the two components of the chlorine doublet gradually merge into a single broad line. The antiresonance above the doublet becomes less distinct and the spectrum smoothly evolves into that of pure KCN. The $A\,^1\Pi$ exciton progression

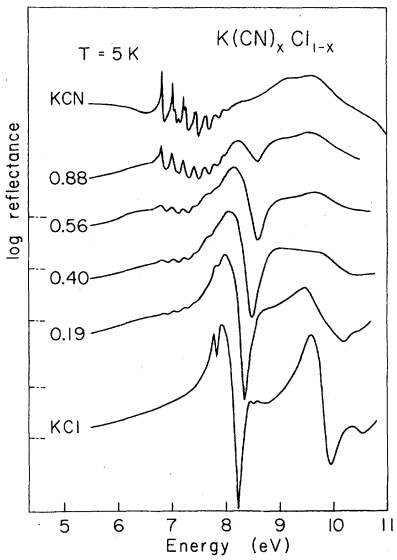

FIG. 8. Reflectance spectra of $K(CN)_x Cl_{1-x}$ mixed crystals at 5 K. The concentration of KCN in the solid solutions is given on the left.

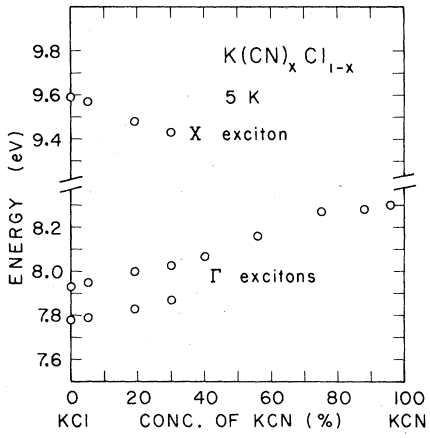

FIG. 9. Positions of the reflectance maxima of the chlorine excitons as a function of concentration in the $K(CN)_xCl_{1-x}$ mixed system.

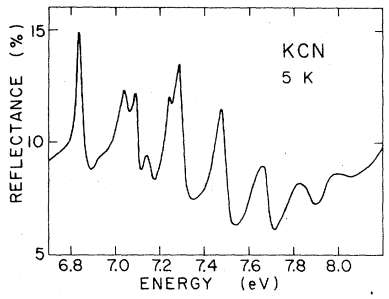

FIG. 10. Reflectance spectrum of the $A\,^1\Pi$ progression in KCN at 5 K (unpolarized light). In this sample a particular domain orientation was favored and therefore a different intensity distribution was observed, as compared with the typical results of Fig. 6.

of CN^- will be discussed in more detail in Sec. VII.

VI. THE $A\,^1\Pi \leftarrow X\,^1\Sigma^+$ EXCITON PROGRESSION IN PURE KCN

A. Experimental results

The reflectance spectrum of Fig. 4 illustrates the effects of the intermolecular interactions upon the $A\,^1\Pi$ excited electronic state of CN^- with its stack of vibrational levels. At 5 K the reflectance bands corresponding to the different vibronic transitions are split into two components. The splitting has been interpreted as a Davydov splitting[36] originating from the resonance interaction between the molecules.[13] Within a single orthorhombic domain one of the two progressions is excited by light polarized along the a axis and the other by light polarized along b. Since the crystals are twinned below 168 K the measured reflectance corresponds to an average over all domain orientations. Hence measurements with polarized light give the same results. In a few samples, however, due probably to strain effects, a particular domain orientation was favored so that a different intensity distribution between the two progressions was observed (Fig. 10).

In a crystal, different types of excited states can result from the vibronic intramolecular excitation. One-particle states occur when the electronic and the vibrational excitation are bound to the same molecule and propagate together as a "vibronic exciton" characterized by the wave vector $\vec{k}$. The transition energies to the one-particle states in KCN are listed in Table III.

TABLE III. Energies of the reflectance maxima in KCN and $K(CN)_xCl_{1-x}$. The second and third columns give the position and width of the peaks in ϵ_2. All values in eV at $T = 5$ K.

	KCN			$K(CN)_xCl_{1-x}$			
				$x = 0.98$	$x = 0.88$	$x = 0.75$	$x = 0.56$
	R	ϵ_2	Γ	R	R	R	R
0-0	6.835	6.840	0.028	6.832	6.832	6.807	6.805
1-0	7.035 7.088	7.043 7.095	0.026 0.032	7.027 (7.082)	7.022	7.009	7.007
2-0	7.240 7.283	7.246 7.290	0.024 0.040	7.235 7.272	7.234	7.223	7.221
3-0	7.441 7.471	7.45 7.482	0.048	7.435 7.464	7.435	7.429	7.426
4-0	7.627 7.662	7.646 7.674	0.070	7.643	7.623		
5-0	(7.780) 7.827	7.85		7.820			
6-0	7.995	8.025		(7.98)			

Within each progression the separation between two successive bands (≈ 0.2 eV) corresponds to the vibrational frequency $\omega_e' = 0.198$ eV of the CN^- molecule in its excited electronic state. Two-particle states are excited states of the crystal in which one vibronic and one purely vibrational excitation propagate separately.[37] The weak reflectance band at 7.14 eV is assigned to such a state. Its separation from the one-particle band at 7.088 eV actually corresponds to the difference $\omega_e'' - \omega_e' = 0.058$ eV between the vibrational frequencies of CN^- in the electronic ground and excited states (Table IV).

The temperature dependence of the reflectance in the 7-eV energy range is important up to 90 K (Fig. 11). With increasing temperature the broadening of the lines lowers the reflectance maxima and obscures the details of the spectra. Above 85 K the band splitting can no longer be observed and the spectra are only weakly temperature dependent. In Fig. 12 the difference between the reflectance values at 6.84 and 6.91 eV (maximum and minimum of the 0-0 band, respectively) is plotted as a function of temperature. The curve indicates that the temperature dependence is mostly confined below 90 K. It provides a convenient comparison between the measured and the calculated spectra.

The real and imaginary parts of the dielectric function $\hat{\epsilon}(\omega)$, deduced from the reflectance spectra taken at 5 K, are drawn in Figs. 13 and 14. Positions and linewidths of the peaks in ϵ_2 are listed in Table III. The functions ϵ_1 and ϵ_2 could

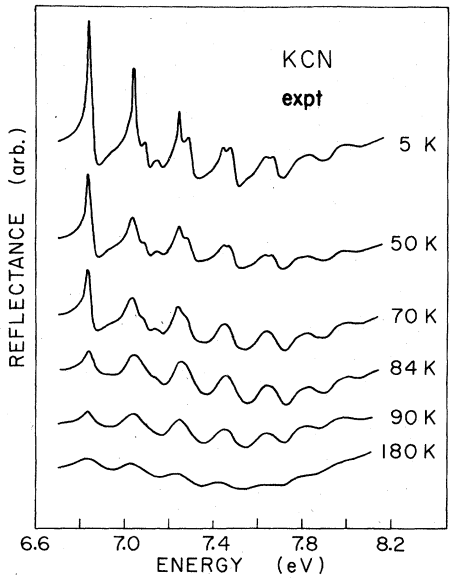

FIG. 11. Reflectance spectrum of the $A\,^1\Pi$ progression in KCN at different temperatures.

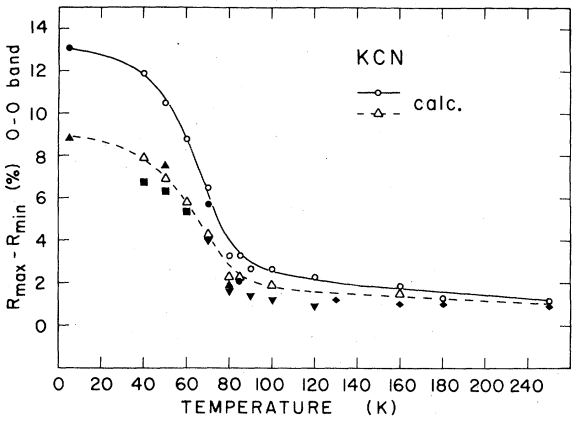

FIG. 12. Difference ΔR between the reflectance values at 6.84 and 6.91 eV (maximum and minimum of the 0-0 band) as a function of temperature, for different samples. The open symbols refer to the reflectance spectra calculated from the $\hat{\epsilon}$ curves of two different samples as described in Sec. VI C. The solid and dashed lines are drawn as a guideline to the eye.

presumably be approximated by a sum of Lorentzians, but in view of the approximations involved in the Kramers-Kronig transformation the values of $\hat{\epsilon}(\omega)$ are uncertain. Therefore a detailed line-shape analysis was not attempted. Nevertheless, since the measured reflectance is reproduced exactly by the expression

$$R = \frac{(\epsilon_1^2+\epsilon_2^2)^{1/2} - 2\{\frac{1}{2}[(\epsilon_1^2+\epsilon_2^2)^{1/2}+\epsilon_1]\}^{1/2}+1}{(\epsilon_1^2+\epsilon_2^2)^{1/2} + 2\{\frac{1}{2}[(\epsilon_1^2+\epsilon_2^2)^{1/2}+\epsilon_1]\}^{1/2}+1}, \qquad (4)$$

the use of $\hat{\epsilon}(\omega)$ in the subsequent analysis is justified.

B. Theory

The theory of light absorption by molecular excitons has been developed by Davydov,[36,38]

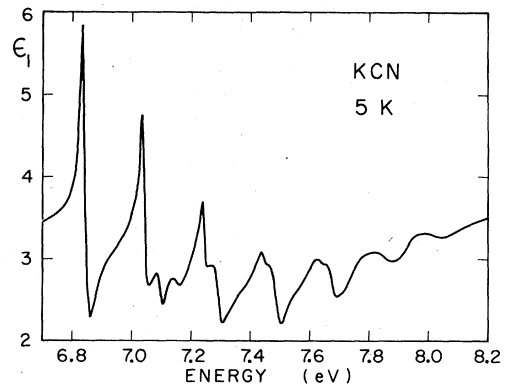

FIG. 13. Dielectric function ϵ_1 of KCN at 5 K as derived from the reflectance data.

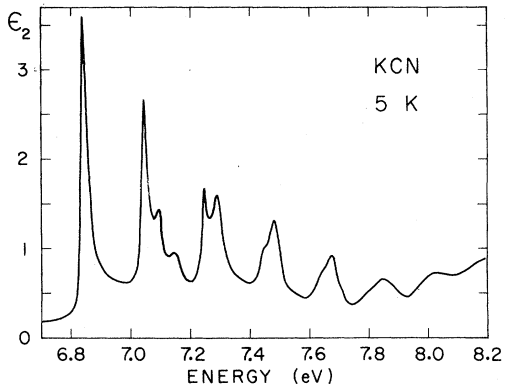

FIG. 14. Dielectric function ϵ_2 of KCN at 5 K, as derived from the reflectance data.

Philpott,[37] and others. Zumofen[39] analyzed in detail the $A\,^1\Pi \leftarrow X\,^1\Sigma^+$ progression in solid CO. A calculation of a synthetic spectrum of the corresponding progression in KCN appeared recently.[13] A brief summary of some theoretical results will be given here.

At 5 K, the CN^- ions are aligned in the lattice with the CN axis lying parallel to the c axis of the orthorhombic cell. The degenerate $A\,^1\Pi$ molecular state splits in the orthorhombic crystal field into two levels, π_x and π_y, with transition dipole moments parallel to the a and b axes.

For the present interpretation it suffices to consider a primitive unit cell containing a single molecule, disregarding whether the orientation is CN or NC. The Hamiltonian of the whole crystal is then

$$H = \sum_n H_n + \sum_{m<n} V_{mn} . \tag{5}$$

H_n is the Hamiltonian of the molecule on site n and includes the effect of the orthorhombic crystal field. V_{mn} is the interaction operator of molecules n and m. We consider for simplicity one-particle states only (vibronic excitons) described by the wave functions

$$\Phi_p^f(\vec{k}) = \frac{1}{\sqrt{N}} \sum_n e^{i\vec{k}\cdot\vec{r}_n} \phi_n^f \chi_{np} \prod_{j\neq n} \phi_j^0 \chi_{j0}^0 . \tag{6}$$

ϕ^f ($f = \pi_x, \pi_y$) are the electronic wave functions of the two excited molecular states; χ_{nq}^0 and χ_{np} are vibrational wave functions of molecule n in its electronic ground and excited state; p and q are vibrational quantum numbers. The ground state of the crystal is given by

$$\Phi^0 = \prod_n \varphi_n^0 \chi_{n0}^0 . \tag{7}$$

In a first step, following Zumofen,[39] the electronic excitation is treated separately from the vibrational problem and the resonance splitting of the electronic transition is calculated. If we consider the two excited states π_x and π_y the electronic resonance interaction matrix takes the form[36]

$$J_{ff'}(\vec{k}) = \sum_m{}' M_{nf,mf'} \exp[i\vec{k}\cdot(\vec{r}_n - \vec{r}_m)] ,$$

where

$$M_{nf,mf'} = \langle \varphi_n^f \varphi_m^0 | V_{nm} | \phi_n^0 \varphi_m^{f'} \rangle$$

are the matrix elements of the transfer of excitation from molecule m to molecule n and the prime on the summation indicates that the term $m = n$ is not summed. If the interaction operator V_{nm} is expanded into a multipole series and only dipole-dipole terms are retained, one obtains

$$J_{ff'}(\vec{k}) = \vec{P}^f \cdot \underline{T}(\vec{k}) \cdot \vec{P}^{f'} ,$$

where $\vec{P}^f$, $\vec{P}^{f'}$ are the transition dipole moments to the states π_x, π_y and

$$\underline{T}(\vec{k}) = \sum_{\vec{R}} R^{-3}(\underline{1} - \hat{R}\hat{R}) \exp(i\vec{k}\cdot\vec{R})$$

is a lattice sum of point dipole-dipole interactions ($\vec{R} = \vec{r}_n - \vec{r}_m$). At the wavelengths of interest, $k \simeq 0$ and the short-range part of the dipole-dipole interaction can be evaluated from the crystal-structure data considering only the molecules within a single crystallographic domain. The short-range interaction leads to the two resonance energies $J_a = t_a P^2$ and $J_b = t_b P^2$ for transition dipoles parallel to the a and b crystal axis, respectively. Here t_a and t_b are dipolar lattice sums and the value of the transition dipole moment has been assumed equal for both states. The above expressions are valid for a medium with a dielectric constant $\epsilon_0 = 1$. For $\epsilon_0 > 1$ we introduce a correction factor $(\epsilon_0+2)^2/9\epsilon_0$, as proposed in Ref. 40, and write

$$J_a = \frac{(\epsilon_0+2)^2}{9\epsilon_0} t_a P^2 , \quad J_b = \frac{(\epsilon_0+2)^2}{9\epsilon_0} t_b P^2 . \tag{8}$$

Next, the long-range (macroscopic) part of the dipole-dipole interaction is computed taking into account the crystallographic domains which are responsible for the mixing of the two electronic states π_x and π_y. In the case of cubic crystals the long-range part of the dipole sum for the transverse exciton is given by[13,41]

$$-\frac{4\pi}{3V}\frac{(\epsilon_0+2)}{3} P^2 , \tag{9}$$

where V is the volume of the unit cell and $(\epsilon_0+2)/3$ is a dielectric correction factor that accounts for the shielding of the long-range interaction due to the influence of the higher transitions. In the case of KCN we assume that the domain distribu-

tion is such that an average cubic symmetry is preserved and that one-third of the transition dipoles are parallel to each cubic axis; thus the long-range part of the interaction becomes $-(4\pi/9V)(\epsilon_0+2)P^2/3$. Finally, the electronic resonance matrix at $\vec{k}=0$,

$$\begin{pmatrix} J_a - \frac{4\pi}{9V}(\epsilon_0+2)\frac{P^2}{3} & -\frac{4\pi}{9V}(\epsilon_0+2)\frac{P^2}{3} \\ -\frac{4\pi}{9V}(\epsilon_0+2)\frac{P^2}{3} & J_b - \frac{4\pi}{9V}(\epsilon_0+2)\frac{P^2}{3} \end{pmatrix} \tag{10}$$

(where $V=\frac{1}{2}abc$) is diagonalized to give the resonance splittings

$$\begin{aligned} J_1 &= \frac{J_a+J_b}{2} - \frac{4\pi}{9V}(\epsilon_0+2)\frac{P^2}{3} \\ &\quad + \left[\left(\frac{J_a-J_b}{2}\right)^2 + \left(\frac{4\pi}{9V}(\epsilon_0+2)\frac{P^2}{3}\right)^2\right]^{1/2}, \\ J_2 &= \frac{J_a+J_b}{2} - \frac{4\pi}{9V}(\epsilon_0+2)\frac{P^2}{3} \\ &\quad - \left[\left(\frac{J_a-J_b}{2}\right)^2 + \left(\frac{4\pi}{9V}(\epsilon_0+2)\frac{P^2}{3}\right)^2\right]^{1/2}. \end{aligned} \tag{11}$$

The data listed in Table IV show that the splitting is mainly due to the long-range interaction. The vibronic interaction matrix

$$\langle \Phi_p^f | H | \Phi_{p'}^{f'} \rangle - \langle \Phi^0 | H | \Phi^0 \rangle$$

can then be reduced to

$$H_{pp'}(J_\mu) = [T^e + G'(p) - G''(0) + D]\,\delta_{pp'} + J_\mu \xi_0^p \xi_0^{p'}, \quad \mu = 1, 2. \tag{12}$$

T^e represents an effective electronic transition energy in the molecule while $G''(q)$ and $G'(p)$ are the vibrational energies in the electronic ground and excited states, respectively. $\xi_0^p = \langle \chi_p | \chi_0^0 \rangle$ are vibrational overlap integrals. The term D stands for the change of the interaction energy of a molecule with all the surrounding molecules due to its excitation:

$$D = \sum_{m\neq 0} \left(\langle \phi_n^f \phi_n^f | V_{nm} | \phi_m^0 \phi_m^0 \rangle - \langle \phi_n^0 \phi_n^0 | V_{nm} | \phi_m^0 \phi_m^0 \rangle \right). \tag{13}$$

TABLE IV. Molecular and crystal constants of KCN (Ref. 13).

Dipole sums	$t_a = -1.01\times10^{22}$ cm^{-3}
	$t_b = 0.24\times10^{22}$ cm^{-3}
Transition dipole moment	$P = 2.74\times10^{-18}$ esu cm
Vibrational constant in the electronic excited state	$\omega_e' = 198.3$ meV
Vibrational constant in the electronic ground state	$\omega_e'' = 256.6$ meV
Dielectric constant	$\epsilon_0 = 1.8$
Effective electronic transition energy	$T^e + D = 6.951$ eV
Resonance splittings	$J_1 = -272$ meV
	$J_2 = -13$ meV

Thus the crystal exhibits two separate vibronic progressions, each described by its own matrix H_μ corresponding to a particular electronic resonance term J_μ. The matrices H_μ can be diagonalized. The transition energies to the vibronic exciton states are given by their eigenvalues $E_{\mu p}$ while the corresponding transition intensities can be derived from their eigenvectors and from the unperturbed one-particle vibronic transition intensities.[13,39] The off-diagonal elements of H_μ modify only weakly the transition energies but strongly affect the intensity distribution.[39] For negative values of the resonance energies J_μ (case of KCN, Table IV) the intensity distribution is shifted towards the lower vibrational bands as compared to the unperturbed distribution in the free molecule. The large difference between J_1 and J_2 explains the different intensity distributions of the corresponding progressions observed in the reflectance and in the ϵ_2 spectrum (Figs. 4 and 14).

The transition energies are approximately given by the diagonal elements of H_μ. Thus the splittings of the vibrational bands

$$\Delta E_p \simeq (J_1 - J_2)(\xi_0^p)^2 \tag{14}$$

vary along the progression to a first order according to the Franck-Condon factors $(\xi_0^p)^2$, as can be seen from the positions of the reflectance maxima (Table III). This indicates that the splittings are essentially due to the resonance interaction between the CN^- molecules.

In order to explain the linewidths of the excitonic structures and the temperature dependence of the reflectance spectrum we must take into account exciton-phonon coupling. A detailed treatment is beyond the scope of this paper and a number of simplifications will be introduced. The exciton-phonon coupling modifies the terms D and J of Eq. (12). The coupling through D is independent of the quantum number p and to first order equal for all bands and for both electronic components:

$$\chi_s(\vec{q}) = \frac{\partial D}{\partial Q_s(\vec{q})} \Delta Q_s(\vec{q}). \tag{15}$$

$Q_s(\vec{q})$ is the phonon normal coordinate with wave vector $\vec{q}$ and branch s and $\Delta Q_s(\vec{q})$ is the corresponding amplitude. It has been shown that this coupling leads to an envelope of multiphonon transitions accompanying the electronic transition.[36]

The width of the envelope is

$$\gamma \sim \sum_{s,\vec{q}} \left(\frac{\chi_s(\vec{q})}{\Omega_s(\vec{q})}\right)^2, \tag{16}$$

where $\Omega_s(\vec{q})$ are the phonon frequencies, and the temperature dependence has been shown to be[36]

$$\gamma \simeq \gamma_0 \coth(\hbar\langle\Omega\rangle/2kT). \tag{17}$$

$\langle\Omega\rangle$ stands for the frequency of the most effective phonons taking part in the transition.

The coupling through the resonance term J can be regarded as a scattering process. Through interactions of the dipole resonance with the phonon field an exciton of energy $E_{\mu\rho}(\vec{k})$ is scattered into another state with energy $E_{\mu'\rho'}(\vec{k}')$. The matrix element for this process, denoted by $F_{s\,\mu\rho,\mu'\rho'}(\vec{k},\vec{q})$, where $\vec{q}$ is the wave vector of the phonon (branch s) involved in the scattering, is approximated by

$$F_{s\,\mu\rho,\mu'\rho'}(\vec{k},\vec{q}) = F_s\,\zeta_{\mu\rho}(\vec{k})\zeta_{\mu'\rho'}(\vec{k}+\vec{q}), \tag{18}$$

where $\zeta_{\mu\rho}(\vec{k})$ are the transformed Franck-Condon factors.[39] Calculations of the coupling functions $F_s(\vec{k},\vec{q})$ show that molecular excitons mainly interact with $\vec{q}\simeq 0$ librational phonons.[36] The reciprocal of the exciton lifetime against such transitions is taken as the optical linewidth[42]:

$$\Gamma_{\mu\rho}(\vec{k}) = 2\pi \sum_{s,q,\mu'\rho'} F_s^2 \zeta_{\mu\rho}^2(\vec{k})\zeta_{\mu'\rho'}^2(\vec{k}+\vec{q}) \times\{[n_s(\vec{q})+1]\delta(\omega_{\mu\rho}(\vec{k}) - \omega_{\mu'\rho'}(\vec{k}+\vec{q}) - \Omega_s(\vec{q})) + n_s(\vec{q})\delta(\omega_{\mu\rho}(\vec{k}) - \omega_{\mu'\rho'}(\vec{k}+\vec{q}) + \Omega_s(\vec{q}))\}, \tag{19}$$

where $n_s(\vec{q}) = [\exp(\hbar\Omega_s(\vec{q})/kT - 1]^{-1}$ is the average number of phonons with frequency $\Omega_s(\vec{q})$ at temperature T. We simplify Eq. (19) to

$$\Gamma_{\mu\rho} = \Gamma_\mu^0 \zeta_{\mu\rho}^2(\vec{k}=0)\coth\left(\frac{\hbar\langle\Omega\rangle}{2kT}\right), \tag{20}$$

with Γ_μ^0 as a constant.

In the following, we assume equal Franck-Condon factors for the most intense bands since we focus our interest less on the quantum number but more on the temperature dependence of the line broadening and recast Eqs. (17) and (20) to

$$\Gamma(T) = (\gamma_0 + \Gamma_0)\coth(\hbar\langle\Omega\rangle/2kT). \tag{21}$$

A coth law for the line broadening has been verified experimentally for phenantrene[43] and KCl (Ref. 44) over a wide temperature range.

The phonon spectrum of KCN has been investigated by infrared and Raman spectroscopy[5,6,45] and by coherent inelastic neutron scattering.[46] The Raman bands observed in the orthorhombic phase below 83 K, centered around 120, 135, 168, and 190 cm^{-1}, have been assigned by Dultz to the librational, the LA, the TO, and LO modes, respectively. In a later paper on the $K(CN)_xCl_{1-x}$ mixed system Durand and Lüty[45] assigned the Raman peaks at 120 and 190 cm^{-1} to two librational modes of the CN^- ions. The phonon density of states obtained from neutron scattering experiments shows at 5 K three peaks attributed to the TA zone-boundary phonons (63 cm^{-1}) and to the Raman-active librational and optical modes (130 and 170 cm^{-1}). With increasing temperature the Raman bands and the peaks in the density of states broaden but remain almost at the same frequencies. The phase transition at 83 K has no important effect upon the phonon spectrum. Therefore one does not expect the exciton-phonon interaction to be much different in the two orthorhombic phases.

C. Temperature dependence of the reflectance spectra

At temperatures above 70 K, where the exciton peaks are broad and the reflectance is low, a satisfactory Kramers-Kronig analysis of the spectra was not possible (see Appendix A). Therefore in the analysis of the temperature dependence of the vibronic progression an indirect approach had to be chosen. In the dielectric function $\hat{\epsilon}(\omega)$ determined from the reflectance at 5 K an additional linewidth γ_{expt} is introduced by folding $\hat{\epsilon}$ with a Lorentzian shape function:

$$\tilde{\epsilon}_i(\omega) = \frac{\gamma_{\text{expt}}}{2\pi}\int_{-\infty}^{+\infty} \hat{\epsilon}_i(\omega')\frac{d\omega'}{\omega'^2 + \frac{1}{4}\gamma_{\text{expt}}^2}, \quad i=1,2. \tag{22}$$

From the functions $\tilde{\epsilon}_i(\omega)$ computed for different values of γ_{expt} reflectance curves are calculated and compared with the experimental results for different temperatures. This computation was performed using the $\hat{\epsilon}$ curves for two samples (solid circles and solid triangles in Fig. 12, respectively) with markedly different reflectances. With the values of γ_{expt} given in Fig. 16 reasonable agreement was obtained as follows:

(i) The overall line shapes reproduce the experimental trend. Below 70 K the resonance splitting is retained, and above 70 K the two Davydov components merge into a series of almost sym-

metric bands.

(ii) The reflectance-versus-temperature curve of Fig. 12 is reproduced fairly well.

This procedure is rather crude and the line shapes of the exciton resonances are now always correctly reproduced. The agreement between calculated and measured spectra is satisfactory throughout the whole energy range only up to about 70 K. Above 80 K some discrepancies become more evident. In particular (Fig. 15), the 0-0 band appears more strongly in the calculated than in the measured spectra, whereas the converse is true for the highest bands. The values of γ_{expt} in Fig. 16 give the best overall agreement, but especially above 80 K their uncertainty is rather large. It must also be noted that the convolution of $\hat{\epsilon}(\omega)$ with a normalized Lorentzian function [Eq. (22)] does not change the intensities of the vibrational bands. Actually, however, if the resonance interaction energies J_μ are modified as the crystal structure and the molecular orientations change with the temperature, a different intensity distribution in the vibrational progression results.

In Fig. 16, the curve

$$\Gamma'(T) = (\Gamma_0 + \gamma_0) + \gamma_{\text{expt}}(T) \tag{23}$$

is compared with the linewidth calculated according to Eq. (21). $\gamma_0 + \Gamma_0 = 30$ meV was taken as a mean linewidth at 5 K (Table III) and the values of $\langle\Omega\rangle = \Omega_{\text{lib}} \simeq 120$ cm^{-1}, given in Ref. 5, were inserted. The temperature dependence of the linewidth cannot be described by a coth law with a single-phonon frequency. $\Gamma'(T)$ increases rapidly in the range from 50 to 100 K and at a much slower rate above 100 K. Since the phonon spectrum remains almost unchanged up to 150 K (Ref. 46), it is difficult to explain this temperature dependence on the basis of exciton-phonon coupling alone. Therefore we suggest that the anomalous line broadening with increasing temperature is due to the onset of orientational disorder in the vicinity of the phase transition at 83 K.[47]

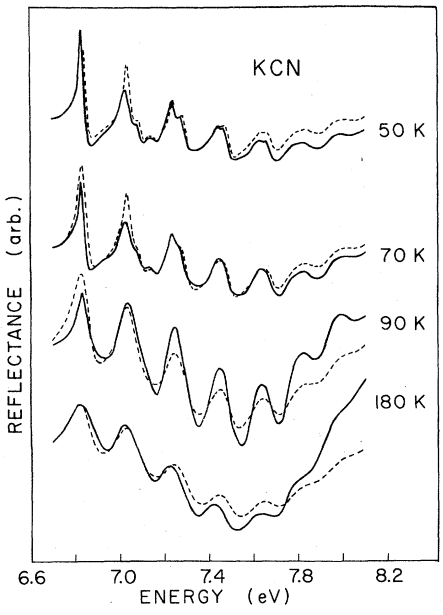

FIG. 15. Solid curves: measured reflectance spectra of KCN at various temperatures. Dashed curves: calculated reflectance spectra as decribed in Sec. VI C. Values of the linewidth parameter γ_{expt} [Eq. (22)] $T = 50$ K, $\gamma_{\text{expt}} = 5$ meV; $T = 70$K, $\gamma_{\text{expt}} = 20$ MeV; $T = 90$ K, $\gamma_{\text{expt}} = 60$ meV; $T = 180$ K, $\gamma_{\text{expt}} = 100$ meV. For the sake of clarity the reflectance values at 90 and 180 K have been multiplied by a constant factor of 3.

D. Diagonal and off-diagonal disorder

In this section the contribution of the diagonal and off-diagonal disorder, originating from molecular orientational disorder, in the line broadening is analyzed. The broadening due to diagonal disorder corresponds to an inhomogeneous line broadening of the diagonal site excitation energy caused by the nonequivalent environments seen by different molecules. Off-diagonal disorder originates from the dependence of the excitation-exchange matrix elements on the relative equilibrium positions of interacting molecules.

Both types of disorder have become of interest in the analysis of excitation transport phenomena in organic molecular crystals.[48] The same basic ideas are applied here to the particular case of orientational disorder. The discussion is restricted to pure dipole-dipole interaction. Numerical results are obtained by simulating the

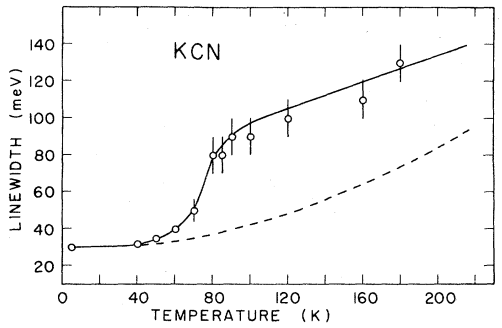

FIG. 16. Average linewidth of the vibrational bands. Solid line: $\Gamma'(T) = (\Gamma_0 + \gamma_0) + \gamma_{\text{expt}}(T)$ from the comparison between the measured and calculated spectra (Fig. 15). $\Gamma_0 + \gamma_0 = 30$ meV. Dashed line: $\Gamma(T)$ according to Eq. (21), linewidth expected from the coupling with the librational phonons.

disorder on a computer.

In a first step we treat the diagonal disorder without considering the resonance interaction between the molecules. As the temperature rises CN^- ions are allowed to flip by 180° but they are kept preferentially aligned along the c axis of the domain as suggested by Suga.[3] This disorder modifies the D term [Eq. (13)] since CN^- has no inversion symmetry, such that for the lattice point n,

$$D_n = \langle D \rangle + \Delta D_n \tag{24}$$

due to the changes in the local environment. The excitation energy of the molecule n is now given by

$$\epsilon = \langle \epsilon \rangle + \Delta D_n , \tag{25}$$

and the linewidth can approximately be written as

$$\Gamma = \Gamma^{\text{ex-ph}} + \Gamma^{\text{disorder}} , \tag{26}$$

with

$$\Gamma^{\text{disorder}} = 2\sigma_D , \tag{27}$$

where σ_D is the width (standard deviation) of the distribution of D_n. The inhomogeneous broadening due to the diagonal disorder is the same for all vibronic bands since D causes a shift of the whole progression. When dipole-dipole interaction only is considered the D term can be written as

$$D = \sum_m{}' \frac{(\vec{p}_0, \vec{\Delta p}_m)}{R_m^3} - 3\frac{(\vec{p}_0, \vec{R}_m)(\Delta\vec{p}_m, \vec{R}_m)}{R_m^5} . \tag{28}$$

$\vec{p}_0$ is the permanent electric dipole moment of the CN^- ion at the origin in the electronic ground state and $\Delta\vec{p}_m$ represents the difference between the dipole moments of the ground and excited electronic states of the ion at site m.

Above 83 K where the probabilities of CN and NC orientations become equal, each term of the sum in Eq. (28) can be taken with a positive or a negative sign. For the computation of the linewidth, the molecules can be assigned to correlation shells around site n. The molecules in a given shell contribute equally to the matrix shift (disregarding the sign). For each shell D_n is binominally distributed. Thus the total linewidth can be easily calculated from the contributions of the shells. We simplified the task by taking a σ_D value computed by taking dipole sums within a sphere of 20-Å radius averaged over many randomly chosen arrangements of CN^- orientations:

$$\sigma_D = 3 \times 10^{22} (\vec{p}_0, \Delta\vec{p}) .$$

With an experimental $\sigma_D \simeq 0.03$ eV at 90 K we obtain $(\vec{p}_0, \Delta\vec{p}) \simeq 1.6 \times 10^{-36}$ esu² cm². A calculation of $(\vec{p}_0, \Delta\vec{p})$ based on theoretical *ab initio* dipole moments for the free CN^- molecule (Table I) results in a much smaller value, namely 1.0×10^{-37} esu² cm². From the discussion in Ref. 49 we believe that the accuracy of the theoretical value is better than a factor 2 such that the discrepancy between the theoretical and experimental results is significant.

At this point the question arises whether the diagonal disorder violates the $\vec{k} \simeq 0$ selection rule such that the band shapes observed above 83 K correspond to the entire exciton band. This question is particularly important in cases where the exciton bandwidth is larger than the Davydov splitting of the $\vec{k} \simeq 0$ frequencies and where the inhomogeneous line broadening is smaller than the exciton bandwidth.

To clarify this point we performed a simple computer simulation. A supercell with cyclic boundary conditions was assumed with dimensions $2a \times 2b \times 2c$ containing 16 molecules and hence 32 dipole transition moments. The CN-NC orientations were chosen in a random manner. A 32×32 resonance matrix was built up with individual matrix shifts added to the diagonal elements. After diagonalization the proper intensities computed by a linear combination of the transition moments with the corresponding eigenvector elements were assigned to the eigenvalues. This was done for one particular vibronic band with an assumed oscillator strength of $f = 0.01$ and *ab initio* electrostatic dipole moments of Table I. This procedure was repeated for several arrangements of molecular orientations in the supercell, and the results with and without resonance interaction were collected in intensity-weighted densities of states which are shown as histograms in Figs. 17(c) and 17(d), respectively. From the comparison with the unperturbed exciton band [Fig. 17(a)] we conclude that the resonance leads to no additional broadening or splitting. The maxima in the spectra appear approximately at the same places as without disorder, and the relative intensity distribution suffers no dramatic change.

It should be emphasized that a pure head-tail disorder causes no off-diagonal disorder, since for resonance dipole-dipole interaction the rotation of one molecule by 180° is equivalent to a phase change of one of the diagonal states. But eigenvalues and intensities are invariant with respect to phase changes, which likewise affect off-diagonal energies, eigenvector elements, and transition moments.[40]

According to Julian[9] and von der Weid *et al.*[11,15] the CN^- ions are reorienting among the [100] and [111] directions when the temperature is raised above 83 K. This type of disorder affects both the shift term D and the resonance term J not only with respect to the signs of the individual con-

tributions but also to their magnitudes.

Including the [111] direction as a possible equilibrium orientation of the molecules in the treatment of the diagonal disorder, it can be easily seen that the broadening is not enhanced since the spread in the matrix shifts is already large when all contributions in Eq. (28) take random signs. Therefore we did not compute the broadening due to this type of diagonal disorder but analyzed the influence of the off-diagonal disorder on the broadening. This was done by means of a computer simulation as described above, i.e., a supercell was taken with molecular orientations distributed statistically among the [100] and [111] directions. The same procedure as discussed above was used to achieve an intensity-weighted density of states which is shown as a histogram in Fig. 17(b). There is only a minor broadening if compared with the unperturbed $\vec{k}=0$ exciton band, and the intensity gained by the high-energy wing is insignificant.

We therefore conclude that the main part of the line broadening is due to the diagonal disorder. Off-diagonal disorder yields only a small enhancement. The frequencies and intensities of the Davydov components are predominantly given by the macroscopic part of the dipole sums which, within a cubic overall symmetry, depend on the mean dipole density alone and which are therefore invariant with respect to the orientational disorder. The final conclusion is that the magnitude of the observed line broadening appearing above 83 K cannot be explained on the basis of dipole-dipole interactions only.

In a preliminary study we have recognized that the quadrupole transition moment is as important as the dipole transition moment in the computation of the Davydov splitting. Combining dipole-dipole and quadrupole-quadrupole interactions, a molecular head-tail disorder suffices to produce a strong off-diagonal disorder which might partly explain the observed broadening. However, from this analysis it cannot be excluded that the line broadening due to the diagonal disorder may dominate through van der Waals or ionic intermolecular interactions not considered here.

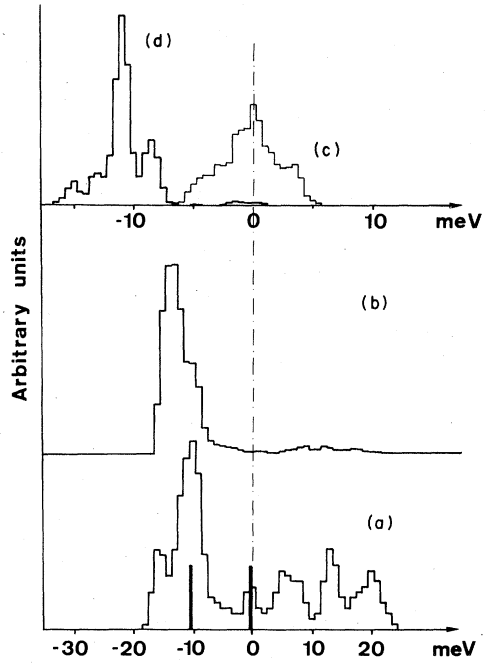

FIG. 17. Diagonal and off-diagonal disorder in KCN. (a) Unperturbed exciton density of states with vertical bars at the two $\vec{k}\simeq 0$ frequencies. (b) Intensity-weighted density of states resulting from off-diagonal disorder when molecular orientations are distributed among [100] and [111] directions. (c) and (d) Intensity-weighted densities of states in the case of diagonal disorder (pure head-tail disorder) without and with resonance interaction, respectively.

VII. THE $A\,^1\Pi \leftarrow X\,^1\Sigma^+$ EXCITON PROGRESSION IN MIXED CRYSTALS

A. Experimental results

It has been emphasized in the preceding section that in pure KCN the $A\,^1\Pi$ progression of exciton states is quite sensitive to orientational disorder. The reflectance spectra of $K(CN)_xCl_{1-x}$ mixed crystals taken at liquid-helium temperature (Fig. 18) demonstrate that substitutional disorder also affects the exciton structures. Even small amounts of Cl^- substituted for CN^- significantly

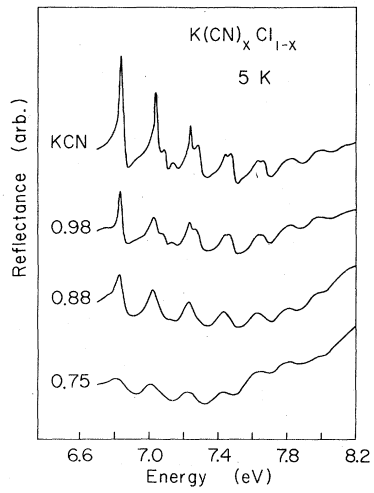

FIG. 18. Reflectance spectra of $K(CN)_xCl_{1-x}$ mixed crystals at 5 K. The cyanide concentration x is given on the left-hand side.

broaden the reflectance peaks.

At low cyanide concentrations ($x<0.6$) the vibronic excitations of CN^- give rise to a series of broad and weak humps superposed on the low-energy tail of the chlorine Γ excitons. No evidence of a band splitting was found. As x is further increased the reflectance bands sharpen and shift slightly toward higher energies (Table III) while the spectrum gradually evolves into that of pure KCN. Above $x=0.90$ the bands become increasingly asymmetric and two separate progressions of vibronic levels can be distinguished. Owing to the large overlap of adjacent bands, an accurate determination of the splittings is still difficult. The observed splittings are only slightly smaller than those of pure KCN. We recall that above $x\approx 0.8$ the crystals break up into domains upon cooling and the reflectance is reduced by light scattering.

Attempts to deduce the complex dielectric function $\hat{\epsilon}(\omega)$ from the reflectance spectra met with limited success. Up to $x\approx 0.8$ the peaks associated with the $A\,^1\Pi$ levels are very weak compared to those due to the chlorine excitons, so that little can be learned from the Kramer-Kronig analysis. For $x\geq 0.9$ the vibronic progression appears with sufficient intensity to allow a reasonably accurate determination of the optical constants.

B. Discussion

In spite of extensive experimental investigations[9,45,50] the behavior of the mixed systems is not yet completely understood. The interpretation of the Raman spectra given by Durand and Lüty, however, provides some information. At the lowest concentrations the CN^- ions substituted into KCl reorient in an octahedral potential with minima along the [111] directions. As x increases the spectra indicate a gradual loss of the [111]-oriented CN^- and a gain of [110]-oriented CN^- ions. For larger x the mixed crystal structure smoothly turns to that of pure KCN.

The effect of successively replacing CN^- by Cl^- ions on the molecular $A\,^1\Pi \leftarrow X\,^1\Sigma$ exciton spectrum can be understood in terms of diagonal and off-diagonal disorder similarly as discussed in the preceding section, where the influence of the phase transition on the linewidth was analyzed. The CN^- ions "see" different environments when neighboring CN^- molecules are statistically replaced by Cl^-, which leads to a change in the diagonal site excitation energy and hence to a diagonal disorder. Off-diagonal disorder occurs since translational symmetry is perturbed when CN^- ions are randomly removed.

The important question is whether diagonal or off-diagonal effects of substitutional disorder dominate the perturbation of the exciton spectrum of pure KCN. Broadening due to diagonal disorder is independent of the vibrational quantum number whereas the one caused by off-diagonal disorder varies from band to band.

Information about the diagonal disorder can be derived from the frequency shift obtained when the Cl^- concentration is increased (Table III). Comparing the reflectance maxima for $x=1$ with those for $x=0.56$, we note a mean frequency shift of approximately 30 meV when the centers of the split bands are considered. It is easy to see that the line broadening originating from the diagonal disorder increases at first linearly with the concentration of Cl^- and reaches a maximum for $x=0.5$, while for $x\approx 0$, the broadening is zero again since CN^- ions are isolated in KCl. As a crude approximation we take the frequency shift of 30 meV at $x=0.56$ as a measure of the maximum broadening and write for the concentration-dependent linewidth $\Gamma(x)\simeq 120x(1-x)$ meV. Discussing now the off-diagonal disorder we write for the resonance energy

$$J_{n\mu}=\langle J\rangle_\mu+\Delta J_{n\mu}\,.$$

Since dipole-dipole interaction varies as r^{-3}, the mean value $\langle J\rangle_\mu$ depends linearly on x. In contrast, the mean standard deviation of the distribution of $\Delta J_{n\mu}$ first increases rapidly when Cl^- is introduced into the lattice, since translational symmetry is violated, but decreases for larger concentrations since the mean dipole density decreases. We estimated the broadening due to the distribution of $\Delta J_{n\mu}$ by summing the contributions of the dipoles within a small sphere choosing the occupation probability of a site at random, but compatible with the concentration x. From averaging over different configurations we found a maximum broadening of approximately 35 meV at $x=0.6$ for a mean Franck-Condon factor of $\zeta=0.25$ and for a dipole moment according to Table IV.

From this we conclude that for the strong bands diagonal and off-diagonal disorders are of the same importance. Spectra of pure KCN folded by Lorentzians [Eq. (22)], using the estimated line broadening, fit the observed broadening in the mixed-crystal spectra satisfactorily. But we note that the band positions and their linewidths are difficult to determine from the experiment since the intensity diminishes and spectral background changes dramatically when the Cl^- concentration is enhanced (Fig. 18). Furthermore, the model describing the off-diagonal disorder is rather crude since it neglects that the $\vec{k}\simeq 0$ selection rule is violated and that a concentration-

dependent intensity redistribution among the vibronic bands should take place. Therefore the discussion of the line broadening in this section is more of a qualitative nature.

VIII. CONCLUDING REMARKS

The $A\,^1\Pi \leftarrow X\,^1\Sigma^+$ transition of the CN^- molecule provides an excellent example for the study of molecular exciton states in solids. The wave functions of localized vibronic excitations constitute a suitable basis set for a quantitative calculation of the $A\,^1\Pi$ progression of vibronic exciton states in the ordered low-temperature phase of pure KCN.[13] The crystal field leads to a perturbation of the $A\,^1\Pi$ state and to a Davydov-type splitting of its vibrational levels.

In order to obtain further information on the effects of structural disorder upon the vibronic exciton states, we have examined the temperature dependence of the $A\,^1\Pi$ progression in pure KCN as well as its concentration dependence in the mixed $K(CN)_xCl_{1-x}$ system. Unfortunately the measurements at low temperature have been hampered by the formation of crystallographic domains that prevented measurements with polarized light and an accurate determination of the transition intensities. Nevertheless, we have shown that in pure KCN important changes in the optical properties occur as a result of order-disorder phase transitions. Diagonal and off-diagonal disorder has been analyzed by a computer simulation on the basis of point-dipole lattices. The study of resonance quadrupole-quadrupole interactions as well as of interactions typical for ionic molecular crystals would give further insight. In the mixed $K(CN)_xCl_{1-x}$ system, the sharp reflectance lines of the $A\,^1\Pi$ exciton resonances are considerably more sensitive to the effects of substitutional disorder than the intense but comparatively broad structures due to the Wannier excitons of chlorine. A rough estimate of the importance of the diagonal and off-diagonal disorder provides a qualitative understanding of the observed broadening in the $A\,^1\Pi$ exciton spectrum in mixed crystals.

ACKNOWLEDGMENTS

We are indebted to Professor K. Dressler and Professor W. Känzig for helpful discussions and for critical reading of the manuscript. This work has benefitted from discussions with Dr. M. Labhart, Dr. M. Stoneham, Dr. M. Ziegler, Dr. M. Rosenfeld, and other members of the Laboratory of Solid State Physics of the ETH. We also thank Mr. H. R. Aeschbach and Mr. M. Wächter for technical assistance. A grant of computer time by the Computer Center of ETH Zürich is gratefully acknowledged. The experimental work was supported by the Swiss National Science Foundation.

APPENDIX: REFLECTANCE MEASUREMENTS AT LOW TEMPERATURES

Some remarks are in order in connection with the reflectance measurements on KCN crystals at low temperatures, i.e., in the orthorhombic multidomain phases. We denote by R and R' the reflectance at room temperature and at 5 K, respectively. The energy dependence of these quantities for the same sample is shown in Fig. 3. At low energies, up to about 6.5 eV, R' is higher than R; then R' decreases gradually and goes through a minimum just below the $A \leftarrow X$ (0-0) absorption edge. Above 8 eV, R' is always lower than R. We believe that this behavior is related to light scattering effects from the domains. In the low-energy range where the absorption coefficient α is low ($\alpha \simeq 10^2$ cm^{-1} at room temperature) the penetration depth of the light wave is larger than the typical domain size (4000 Å, Ref. 3), and multiple reflections at the domain boundaries within the crystal can lead to an effective enhancement of the reflectance.[51] In the absorption region above 7 eV, where $\alpha \simeq 10^5$ cm^{-1} at room temperature, multiple reflections within the bulk will not occur and moreover the reflectance is reduced by diffuse light scattering from the rough surface. At the same time the absolute values of R' vary from sample to sample. Peak values ranging from 0.12 to 0.18 have been measured at 6.85 eV (0-0 band). All these effects make a proper normalization of the low-temperature data practically impossible.

As previously noted, the Kramers-Kronig analysis of the uncorrected spectrum often yields negative values of ϵ_2. Therefore in order to obtain a physically meaningful estimate of $\hat{\epsilon}(\omega)$ we have constructed a reflectance curve $R'(E)$ using measurements on different samples. In the range of the $A \leftarrow X$ transition the data refer to a sample that was also measured at 70 and at 84 K (full circles in Fig. 12); above 8 eV the values of R' were taken from a different sample and scaled up by a factor of 1.6 to obtain a continuous curve; finally below 6.5 eV the room-temperature values of R were used, appropriately shifted. The dielectric function $\hat{\epsilon}$ derived from this curve (Figs. 6, 13, and 14) is representative of KCN although the absolute values of R', ϵ_1, and ϵ_2 have limited significance. In fact, except for a few exceptional cases (Fig. 10), the R' and $\hat{\epsilon}$ spectra of different samples in the region above 6.5 eV are proportional, i.e., the positions and linewidths of the

different bands are the same.

A calculation of the oscillator strength

$$n_{\text{eff}} = \frac{2mV_0}{e^2h^2}\int_0^{E'} E\epsilon_2(E)\,dE,$$

with $E' = 11.5$ eV, from the ϵ_2 curves of Figs. 5 and 6 yields $n_{\text{eff}} = 1.88$ at 300 K and $n_{\text{eff}} = 2.06$ at 5 K. Apparently the reflectance R' has been slightly overestimated. In view of this, the computation described in Sec. VI C has been performed using the $\hat{\epsilon}$ curves for two samples with markedly different reflectances. The corresponding values of n_{eff} at 11.5 eV were 2.06 and 1.63, respectively. In spite of these differences the temperature dependence of the reflectance for both samples can be reproduced with the same values of the linewidth parameter γ_{expt}.

---

*Present address: Department of Physics, Indiana University, Bloomington, Indiana 47405.

†Present address: Bell Laboratories, Holmdel, New Jersey 07733.

[1]J. M. Bijvoet and J. A. Lely, Recl. Trav. Chim. Pays-Bas 59, 908 (1940).

[2]A. Cimino, G. S. Parry, and A. R. Ubbelohde, Proc. R. Soc. London Ser. A 252, 445 (1959).

[3]H. Suga, T. Matsuo, and S. Seki, Bull. Chem. Soc. Jpn. 41, 583 (1968).

[4]J. M. Rowe, D. G. Hinks, D. L. Price, S. Susman, and J. J. Rush, J. Chem. Phys. 58, 2039 (1973).

[5]W. Dultz, Solid State Commun. 15, 595 (1974).

[6]W. Dultz, J. Chem. Phys. 65, 2812 (1976).

[7]S. Haussühl, Solid State Commun. 13, 147 (1973).

[8]W. Rehwald, J. R. Sandercock, and M. Rossinelli, Phys. Status Solidi A 42, 699 (1977).

[9]M. D. Julian, Ph. D. dissertation, University of Utah, Salt Lake City, Utah, 1976 (unpublished); M. D. Julian and F. Lüty, Ferroelectrics 16, 201 (1977).

[10]J. M. Rowe, J. J. Rush, and E. Prince, J. Chem. Phys. 66, 5147 (1977); J. M. Rowe, J. J. Rush, E. Prince, and N. J. Cherrer, Ferroelectrics 16, 107 (1977).

[11]J. P. von der Weid, L. C. Scavarda do Carmo, R. R. dos Santos, B. Koiller, S. Costa Ribeiro, and A. S. Chaves, J. Phys. (Paris) 37, C7-241 (1976).

[12]M. A. Bösch and M. Rossinelli, Bull. Am. Phys. Soc. 21, 590 (1976).

[13]M. A. Bösch and G. Zumofen, Phys. Rev. Lett. 41, 590 (1978).

[14]K. H. Michel and J. Naudts, J. Chem. Phys. 67, 547 (1977).

[15]R. R. dos Santos, B. Koiller, J. P. von der Weid, S. Costa Ribeiro, A. S. Chaves, and F. C. Sa Barreto, J. Phys. C 11, 4557 (1978).

[16]M. Bösch and W. Känzig, Helv. Phys. Acta 48, 743 (1975).

[17]E. Boursey, V. Chandrasekharan, P. Günter, E. E. Koch, P. Kunsch, and V. Saile, Phys. Rev. Lett. 41, 1516 (1978).

[18]S. R. Scharber, Jr. and S. E. Webber, J. Chem. Phys. 55, 3977 (1971).

[19]D. M. Roessler, Br. J. Appl. Phys. 16, 1119 (1965).

[20]R. Klucker and U. Nielsen, Comput. Phys. Commun. 6, 187 (1973).

[21]F. Bassani and G. Pastori Parravicini, *Electronic States and Optical Transitions in Solids* (Pergamon, Oxford, 1975).

[22]C. Bradley and A. Cracknell, *The Mathematical Theory of Symmetry in Solids* (Clarendon, Oxford, 1972).

[23]J. B. Moffat, J. Mol. Struct. 25, 303 (1975).

[24]R. Bonaccorsi, C. Petrongolo, E. Scrocco, and J. Tomasi, Chem. Phys. Lett. 3, 473 (1969).

[25]D. N. Hendrickson and P. M. Kuznesof, Theor. Chim. Acta 15, 57 (1969).

[26]T. Yonezawa, H. Kato, and H. Konishi, Bull. Chem. Soc. Jpn. 40, 1071 (1967).

[27]G. Herzberg, *Spectra of Diatomic Molecules* (Van Nostrand, New York, 1950).

[28]E. von der Heyden and F. Fischer, Phys. Status Solidi B 69, 63 (1975).

[29]A. S. Koster, Chem. Phys. Lett. 23, 18 (1973).

[30]W. H. Morrison and D. N. Hendrickson, Inorg. Chem. 11, 2600 (1972).

[31]M. Considine, J. A. Connor, and I. H. Hillier, Inorg. Chem. 16, 1392 (1977).

[32]Y. Onodera and Y. Toyozawa, J. Phys. Soc. Jpn. 24, 341 (1968).

[33]T. Murata, J. Phys. Soc. Jpn. 25, 1632 (1968).

[34]G. Baldini and B. Bosacchi, Phys. Rev. 166, 863 (1968).

[35]D. M. Roessler and W. C. Walker, Phys. Rev. 166, 599 (1968).

[36]A. S. Davydov, *Theory of Molecular Excitons* (Plenum, New York, 1971).

[37]M. R. Philpott, J. Chem. Phys. 55, 2039 (1971).

[38]A. S. Davydov and E. N. Myasnikov, Phys. Status Solidi 20, 153 (1967).

[39]G. Zumofen, Ph. D. dissertation, ETH Zürich, 1976 (unpublished); G. Zumofen and K. Dressler, *XIth European Congress on Molecular Spectroscopy, Tallinn, USSR*, 1973 (Acad. Sci., Estonian SSR, Tallinn, USSR, 1972).

[40]G. Zumofen, J. Chem. Phys. 68, 3747 (1978).

[41]M. R. Philpott, J. Chem. Phys. 56, 591 (1971).

[42]R. S. Knox, *Theory of Excitons*, Solid State Physics (Academic, New York, 1963), Suppl. 5.

[43]A. S. Krochuk and E. V. Smishko, Opt. Spectrosk. 39, 1098 (1975).

[44]T. Tomiki, J. Phys. Soc. Jpn. 26, 738 (1969).

[45]D. Durand and F. Lüty, Ferroelectrics 16, 205 (1977).

[46]N. Nücker, K. Knorr, and H. Jex, J. Phys. C 11, 1 (1978).

[47]J. Klafter and J. Jortner, J. Chem. Phys. 68, 1513 (1978).

[48]J. Klafter and J. Jortner, J. Chem. Phys. 71, 1961 (1979).

[49]T.-K. Ha and G. Zumofen, Mol. Phys. 40, 445 (1980).

[50]J. C. Castro and M. de Suza, Phys. Status Solidi B 86, 137 (1978).

[51]I. Filinski, Phys. Status Solidi B 49, 577 (1972).